Single-Source Three-Phase Multilevel Inverter Assembled by Three-Phase Two-Level Inverter and Two Single-Phase Cascaded H-Bridge Inverters

Tohid Qanbari and Behrouz Tousi

***Abstract*—Multilevel inverters (MLIs) with reduced number of switching devices and dc sources have compact size, reduced cost, and higher efficiency. This article proposes a transformer-based single-source MLI with reduced number of components and small size transformers. The proposed topology is a hybrid three-phase MLI assembled by a conventional three-phase two-level inverter (TTI) and two single-phase cascaded H-bridge inverters (CHBIs). The proposed MLI has a low ratio of number of active switches to number of output voltage levels. In order to use only one dc source, the CHBIs are cascaded with the TTI through transformers. An individual nearest level modulation (NLM) has been developed to control voltage of this inverter. Moreover, power distribution between its modules is analyzed. The total power of the transformers is 28% of the inverter rated power. Simulation and experimental results of a 13-kVA prototype verify the efficiency of the proposed arrangement.**

***Index Terms*—Cascaded H-bridge inverter, hybrid inverter, multilevel inverter, nearest-level modulation, three-phase two-level inverter.**

I. Introduction

MULTILEVEL inverters (MLIs) are the advanced and modern category of dc to ac converters. Compared with two-level inverters, MLIs have significant advantages including quasi-sinusoidal output voltage (with lower THD and improved harmonic spectrum), higher power and voltage capability, lower switching losses, lower *dv/dt*, and reduced common-mode voltage [1], [2]. However MLIs have some drawbacks, such as large number of power semiconductor switches, requirement for multiple of dc sources, and complexity [1], [2]. Cost, number of components, size, and complexity of an inverter are proportional to the number of its switches and sources. Research works for the innovation of topologies with reduced number of switches and sources are very important and beneficial.

In order to remedy the mentioned drawbacks, numerous effective solutions have been proposed and developed. A nine-level switched-capacitor-based topology with reduced number of components has been proposed in [3]. The proposed MLI in [4] is an optimized topology for five or higher level operation, which consists of two basic units of multilevel converter and a T-structured three-level inverter. A new MLI topology based on multilevel dc-link stage has been presented in [5]. A novel three-phase hybrid cascaded MLI using level-doubling network modules with 1:7 ratio of asymmetry is proposed in [6]. A single-source five-level MLI topology with reduced number of floating capacitors and switches has been proposed in [7] for open-end induction motor drives. The hybrid asymmetric cascaded MLIs proposed in [8] consist of a three-level H-bridge cell and a modular nine-level H-bridge cell connected in series. A new three-phase seven-level inverter topology is presented in [9], which is a combination of two cascade-connected two-level inverters and H-bridge cells with flying capacitors. A novel single-source five-level three-phase MLI consisting a two-phase converter and a Scott-T transformer has been proposed in [10]. The five-level converter generates only two-phase voltages. Later, these voltages are converted into three phases by using the Scott-T transformer connection.

One of the major limitations in most of MLI topologies is the requirement of multiple of isolated dc voltage sources. Specially, in some applications, the sources need to be regenerative and costly regenerative rectifiers have to be implemented. The requirement for various dc sources increases complexity, cost, components and bulk of the overall system, and reduce efficiency and reliability [11], [12]. Utilizing of transformers is one of the effective solutions for using only one dc source in MLIs [13]–[22]. Attractive transformer-based single-source MLI topologies have been proposed recently in literature. Cascaded connection of H-bridge cells through single-phase transformers is proposed in [14] and [15]. Single-source three-phase CHBIs using three-phase transformers have been proposed in [16] and [17]. In [18], the combination in CHBIs based on transformers with the different turn ratios for increasing the voltage level is analyzed and the switching method for achieving the output voltage distribution among H-bridge cells is proposed. Efficient transformer-based single-source MLI topologies with reduced components have been proposed in [19]–[21].

Transformer-based topologies utilize low-frequency transformers with total rated power equal with rated power of inverter. The use of a number of transformers in these topologies increases the cost, weight, and size of the overall system. The main challenge of these topologies is to reduce the number and size of

Manuscript received February 23, 2020; revised June 13, 2020 and August 14, 2020; accepted September 26, 2020. Date of publication October 9, 2020; date of current version January 22, 2021. Recommended for publication by Associate Editor *H. L. Ginn. (Corresponding author: Behrouz Tousi.)*

The authors are with the Electrical Engineering, Urmia University, Urmia 5756151818, Iran (e-mail: t.qanbari@urmia.ac.ir; b.tousi@urmia.ac.ir).

Color versions of one or more of the figures in this article are available online at https://ieeexplore.ieee.org.

Digital Object Identifier 10.1109/TPEL.2020.3029870

the transformers [17], [22]. Moreover, they cannot operate at a wide range of frequencies because of the transformers saturation and losses. A single-source binary asymmetric CHBI with small size transformers has been proposed in [22]. The transformer of the main H-bridge that supplies a major part of the output power has been eliminated in this topology. An attractive solution for using only one dc source in MLIs is to utilize high-frequency transformer at dc side instead of low-frequency transformers at ac side [11], [23], [24]. The high-frequency transformer provides multiple of isolated dc sources in these topologies. Besides the use of low-size and low-cost transformer, there is no frequency range limitation in output voltage of these MLIs.

An interesting group of MLI topologies are hybrid inverters. Hybrid MLIs combine distinct switches, topologies, and modulation strategies to optimize the power processing. High number of voltage levels with reduced number of isolated dc sources and switches, reduced conduction and switching losses, and reduced harmonics contents are the advantages of these inverters [4], [16], [25]. An improved three-phase hybrid MLI is the ac-side cascaded topology of TTI with H-bridge or half-bridge inverters. Commonly, TTI is the main power module that controls the fundamental voltage and the cascaded submodules represent a series of active filter in these topologies [26]. Cascaded connection of TTI and H-bridge modules has been proposed in [27]–[29]. TTI and each of the H-bridge converters are supplied by separated dc sources in these inverters. In the MLI proposed in [30], TTI is cascaded with half-bridge submodules. A novel configuration has been proposed in [31]. One H-bridge inverter and one or more auxiliary half-bridge modules are cascaded with a TTI in each phase in this topology.

A novel cascaded topology of TTI and CHBIs is proposed in this article. The TTI is cascaded with CHBIs at two of the phases (phase *a* and *c*) instead of triple of the phases in this inverter. The TTI and the H-bridge modules are connected in ac sides through transformers and supplied by common dc source. The proposed inverter is a hybrid MLI with reduced number of components (active switches, driving circuitry, etc.), single dc source, and small size transformers. Voltage control of the proposed inverter can be carried out by conventional modulation techniques. An individual nearest level modulation for the proposed inverter is presented in this article. Moreover, the power distribution in this inverter is analyzed. A 13-kVA prototype has been simulated and implemented. Simulation and experimental results demonstrate appropriate performance of the proposed topology.

II. Proposed MLI Topology

A. Topology

To achieve an improved harmonics spectrum and THD in TTIs, this inverter operates by PWM methods with high switching frequencies and utilizes passive filters at output terminals. However, as the switching frequency of an inverter increases, its switching losses increase. In order to increase the efficiency and improve harmonics spectrum and THD, a solution is the utilizing of active filters at TTI output. An auxiliary MLI, such as cascaded H-bridge inverter, is connected to TTI in these topologies [26]–[31]. Generally, TTI operates in square-wave mode (with high efficiency) and the auxiliary units increase the number of voltage levels in these topologies. The proposed MLI has such structure. This inverter topology is shown in Fig. 1. A TTI is cascaded with two single-phase CHBIs through transformers at phases *a* and *c*. The CHBIs may contain one or more three-level H-bridge modules. All of the modules (the TTI and the H-bridges) are supplied by a single dc source. This is a hybrid topology of CHBI and TTI.

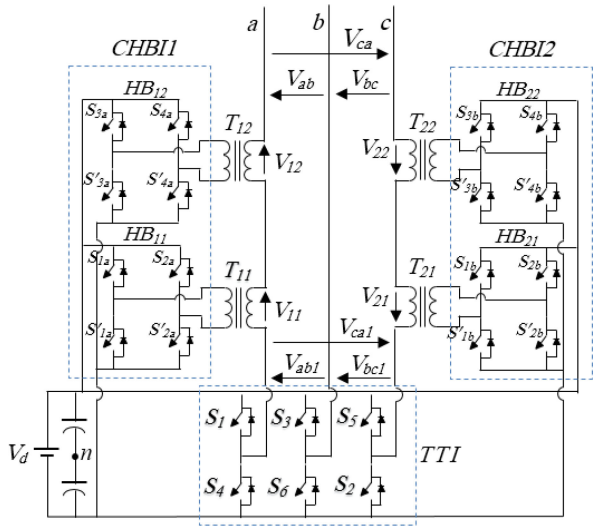

Fig. 1. Proposed hybrid three-phase MLI assembled by a TTI and two single-phase CHBIs.

By the proper selection of the transformers turns ratios, the inverter may be symmetrical or asymmetrical. Trinay asymmetrical topology can synthesize the most output voltage levels and then it is the most appropriate topology in the case of asymmetric condition [11], [14], [32]. Trinay structure of this MLI is considered in this article. Therefore, the turns ratios of T_{11} and T_{21} are 3:1 and the turns ratios of T_{12} and T_{22} are 9:1. It will be shown that the TTI supplies a major part of output power and the H-bridge modules and the transformers in this topology are low-rating and small size H-bridge modules and transformers.

B. Output Voltage

The line *a* to line *b* voltage (V_{ab}) in the proposed inverter is sum of the *ab* line voltage (V_{ab1}) of the TTI and the output voltage of the CHBI1. With two H-bridge modules in each CHBI (Fig. 1), this voltage is

$$V_{ab} = V_{ab1} + V_{11} + V_{12} \tag{1}$$

where V_{11} and V_{12} are the secondary sides voltages of T_{11} and T_{12}, respectively. Similarly, the line *b* to line *c* voltage (V_{bc}) of the inverter is sum of the *bc* line voltage (V_{bc1}) of the TTI and the output voltage of the CHBI2. With two H-bridge modules, this voltage is

$$V_{bc} = V_{bc1} + V_{21} + V_{22} \tag{2}$$

TABLE I
SWITCHING STATES OF THE TTI

A_{ab1}	A_{bc1}	Switching States
V_d	0	S_1, S_2, S_6
V_d	$-V_d$	S_1, S_5, S_6
0	V_d	S_1, S_2, S_3
0	0	S_1, S_3, S_5 or S_2, S_4, S_6
0	$-V_d$	S_4, S_5, S_6
$-V_d$	V_d	S_2, S_3, S_4
$-V_d$	0	S_3, S_4, S_5

where V_{21} and V_{22} are the secondary sides voltages of T_{21} and T_{22}, respectively. Considering V_{ab} and V_{bc} pure sinusoidal voltages as follows:

$$V_{ab} = V_m \sin(\omega t) \tag{3}$$

$$V_{bc} = V_m \sin(\omega t - 120^\circ). \tag{4}$$

V_{ca} will be

$$V_{ca} = -(V_{ab} + V_{bc}) = -V_m [\sin(\omega t) + \sin(\omega t - 120^\circ)]$$
$$= V_m \sin(\omega t + 120^\circ) \tag{5}$$

where V_m is the amplitude and ω is the angular velocity of the voltages. Equations (3)–(5) show that V_{ab}, V_{bc}, and V_{ca} are balanced three-phase voltages at the a, b, and c terminals. In other words, by two sinusoidal or quasi-sinusoidal voltages with 120° phase shift, balanced three-phase voltages can be achieved in the inverter output terminals.

The commutation technique more appropriated for this MLI is the NLM [11], [23], [33]. An individual NLM technique has been developed for this MLI. In accordance with the inverter structure, the NLM method has two reference voltages as follows:

$$v_{rab1} = mV_d \sin(\omega t) \tag{6}$$

$$v_{rbc1} = mV_d \sin(\omega t - 120^\circ) \tag{7}$$

where m is the modulation index, V_d is the dc source voltage, and v_{rab1} and v_{rbc1} are the references for line a to line b (V_{ab}) and line b to line c (V_{bc}) voltages, respectively. Switching pattern for the TTI is obtained by comparisons of these reference signals with two constant values given by

$$c_{p1} = -c_{n1} = \frac{V_d}{2}. \tag{8}$$

Results of these comparisons are two rectangular signals that specify waveforms of the line a to line b voltage (V_{ab1}) and the line b to line c voltage (V_{bc1}) of the TTI. The rectangular signal corresponding to V_{ab1} has the below equation:

$$A_{ab1} = \begin{cases} V_d, & v_{rab1} \geq c_{p1} \\ 0, & v_{rab1} < c_{p1} \text{ or } v_{rab1} > c_{n1} \\ -V_d, & v_{rab1} \leq c_{n1}. \end{cases} \tag{9}$$

Replacing v_{rab1} with v_{rbc1} in the above equation gives the rectangular signal corresponding to V_{bc1} (A_{bc1}). Table I lists the switching states of the TTI for different values of A_{ab1} and A_{bc1}. Fig. 2 shows the waveforms of the voltage references, gate pulses of the TTI switches obtained by the mentioned comparisons, and the output voltages of the TTI for $m = 1$.

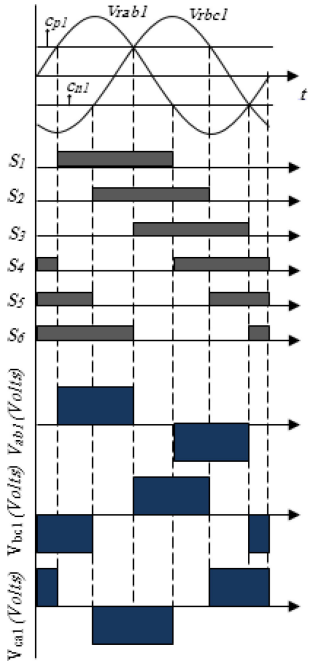

Fig. 2. Waveforms of the voltage references, gate pulses of the TTI switches, and the output voltages of the TTI for $m = 1$.

Modulation of the H-bridge cells has the above algorithm too. The modulation signal for the CHBIs is the difference between the reference voltage and the TTI output voltage. Voltage references of $HB_{1(i)}$ in the CHBI1 is

$$v_{rab(i+1)} = v_{rab(i)} - A_{ab(i)} \qquad i = 1, 2, 3, \ldots \tag{10}$$

where generally

$$A_{ab(i+1)} = \begin{cases} \frac{V_d}{3^i}, & v_{rab(i+1)} \geq c_{p(i+1)} \\ 0, & v_{rab(i+1)} < c_{p(i+1)} \text{ or } v_{rab(i+1)} > c_{n(i+1)} \\ -\frac{V_d}{3^i}, & v_{rab(i+1)} \leq c_{n(i+1)} \end{cases} \tag{11}$$

where

$$c_{p(i+1)} = -c_{n(i+1)} = \frac{V_d}{2 \times 3^i}. \tag{12}$$

Fig. 3 shows the modulation algorithm graphically for $m = 1$ in the interval $0 \leq \omega t \leq \pi/2$, and Fig. 4 shows the output voltages of the TTI, HB_{11}, and HB_{12} (V_{ab1}, V_{11}, and V_{12}) and also V_{ab} in the interval $0 \leq \omega t \leq \pi/2$ for $m = 1$.

The number of output voltage levels of the inverter (the line voltages and the phases a and c voltages with respect to the imaginary neutral point o) is

$$N = 2 \times 3^H + 1 \tag{13}$$

where H is the number of H-bridge modules in each CHBI. Value of each step of the output voltage is

$$E = \frac{2V_d}{(N-1)}. \tag{14}$$

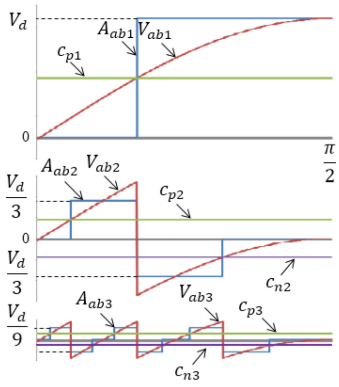

Fig. 3. Graphical illustration of the nearest level modulation for the proposed hybrid MLI in the CHBI1 for $m = 1$.

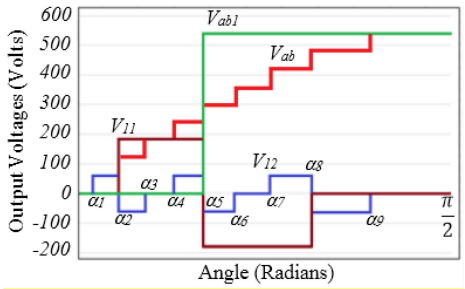

Fig. 4. Output voltages of the TTI and the H-bridges in the CHBI1 of the proposed MLI and V_{ab}.

For $H = 2$ (Fig. 1), the output voltage of the MLI is a 19-level voltage with steps equal with V_d/9. Values of α angles in the waveforms shown in Fig. 4 depend on the m value. The relationship between these angles and the m value is

$$\alpha_k = \arcsin\left(\frac{2k-1}{(N-1)\,m}\right), \quad k = 1, 2, 3, \ldots, \frac{(N-1)}{2}. \tag{15}$$

The values of c_{pi} and c_{ni} are selected according to this equation for $m = 1$. For example, α_5 for $m = 1$ is 30°. Then, the of c_{p1} with the reference signal occurs at 30°. On the other hand, the peak value of the reference signal is V_d. So, the value of c_{p1} must be V_d sin 30°. Obviously, the modulation of the H-bridge cells in the CHBI2 has the same algorithm with only a 120° phase shift. Table II lists the switching states of the H-bridge modules to synthesize V_{ab} and V_{bc}.

C. Power Analysis

One of the most important aspects in the design and analysis of the proposed hybrid MLI is to determine the power distribution among the modules in terms of modulation index.

The power distribution varies by the variation of modulation index. The output voltages and currents can be assumed sinusoidal in this analysis. So

$$V_{ab}(t) = mV_d \sin(\omega t) \tag{16}$$

$$I_a(t) = I_m \sin\left(\omega t - \varphi - \frac{\pi}{6}\right) \tag{17}$$

TABLE II
SWITCHING STATES OF THE H-BRIDGE MODULES

A_{ab2} or A_{bc2}	A_{ab3} or A_{bc3}	*Switching States of CHBI1*	*Switching States of CHBI2*	V_{ab} or V_{bc}
0	0	S_{1a}, S_{2a}, S_{3a}, S_{4a}	S_{1b}, S_{2b}, S_{3b}, S_{4b}	+9E
0	-E	S_{1a}, S_{2a}, S'_{3a}, S_{4a}	S_{1b}, S_{2b}, S'_{3b}, S_{4b}	+8E
-3E	+E	S'_{1a}, S_{2a}, S_{3a}, S'_{4a}	S'_{1b}, S_{2b}, S_{3b}, S'_{4b}	+7E
-3E	0	S'_{1a}, S_{2a}, S_{3a}, S_{4a}	S'_{1b}, S_{2b}, S_{3b}, S_{4b}	+6E
-3E	-E	S'_{1a}, S_{2a}, S'_{3a}, S_{4a}	S'_{1b}, S_{2b}, S'_{3b}, S_{4b}	+5E
+3E	+E	S_{1a}, S'_{2a}, S_{3a}, S'_{4a}	S_{1b}, S'_{2b}, S_{3b}, S'_{4b}	+4E
+3E	0	S_{1a}, S'_{2a}, S_{3a}, S_{4a}	S_{1b}, S'_{2b}, S_{3b}, S_{4b}	+3E
+3E	-E	S_{1a}, S'_{2a}, S'_{3a}, S_{4a}	S_{1b}, S'_{2b}, S'_{3b}, S_{4b}	+2E
0	+E	S_{1a}, S_{2a}, S_{3a}, S'_{4a}	S_{1b}, S_{2b}, S_{3b}, S'_{4b}	+E
0	0	S_{1a}, S_{2a}, S_{3a}, S_{4a}	S_{1b}, S_{2b}, S_{3b}, S_{4b}	0
0	-E	S_{1a}, S_{2a}, S'_{3a}, S_{4a}	S_{1b}, S_{2b}, S'_{3b}, S_{4b}	-E
-3E	+E	S'_{1a}, S_{2a}, S_{3a}, S'_{4a}	S'_{1b}, S_{2b}, S_{3b}, S'_{4b}	-2E
-3E	0	S'_{1a}, S_{2a}, S_{3a}, S_{4a}	S'_{1b}, S_{2b}, S_{3b}, S_{4b}	-3E
-3E	-E	S'_{1a}, S_{2a}, S'_{3a}, S_{4a}	S'_{1b}, S_{2b}, S'_{3b}, S_{4b}	-4E
+3E	+E	S_{1a}, S'_{2a}, S_{3a}, S'_{4a}	S_{1b}, S'_{2b}, S_{3b}, S'_{4b}	-5E
+3E	0	S_{1a}, S'_{2a}, S_{3a}, S_{4a}	S_{1b}, S'_{2b}, S_{3b}, S_{4b}	-6E
+3E	-E	S_{1a}, S'_{2a}, S'_{3a}, S_{4a}	S_{1b}, S'_{2b}, S'_{3b}, S_{4b}	-7E
0	+E	S_{1a}, S_{2a}, S_{3a}, S'_{4a}	S_{1b}, S_{2b}, S_{3b}, S'_{4b}	-8E
0	0	S_{1a}, S_{2a}, S_{3a}, S_{4a}	S_{1b}, S_{2b}, S_{3b}, S_{4b}	-9E

where φ is the angle of the load impedance. The rated power of the inverter is

$$P_n = \sqrt{3}\, V_L I_\varphi \cos\varphi = \sqrt{3}\, \frac{V_d}{\sqrt{2}} I_\varphi \cos\varphi \tag{18}$$

where V_L and I_φ are the nominal rms values of line-to-line output voltage and phase current, respectively.

The output voltages of the converters can be expressed using Fourier decomposition as follows:

$$V_{ab1} = \frac{4\,V_d}{\pi} \sum_{n=1}^{\infty} \frac{1}{n} \cos(n\alpha_5) \sin(n\omega t), \quad n = 1,\ 3,\ 5, \ldots \tag{19}$$

$$V_{11} = \frac{4\,V_d}{3\pi} \sum_{n=1}^{\infty} \frac{1}{n} \left[\cos(n\alpha_2) + \cos(n\alpha_8) - 2\cos(n\alpha_5)\right] \sin(n\omega t), \quad n = 1,\ 3,\ 5,\ \ldots \tag{20}$$

$$V_{12} = \frac{4\,V_d}{9\pi} \sum_{n=1}^{\infty} \frac{1}{n} \lambda \sin(n\omega t), \qquad n = 1,\ 3,\ 5, \ldots \tag{21}$$

where

$$\lambda = \begin{bmatrix} (\cos(n\alpha_1) + \cos(n\alpha_3) - 2\cos(n\alpha_2)) + \\ (\cos(n\alpha_4) + \cos(n\alpha_6) - 2\cos(n\alpha_5)) + \\ (\cos(n\alpha_7) + \cos(n\alpha_9) - 2\cos(n\alpha_8)) \end{bmatrix}.$$

Only the fundamental harmonics of the voltages and currents contribute in supplying the output power. The active power of the TTI is

$$P_{\mathrm{TTI}} = \sqrt{3}\, \frac{V_{ab1(1)}}{\sqrt{2}} I_a \cos\varphi = \sqrt{3}\, \frac{\frac{4\,V_d}{\pi} \cos(\alpha_5)}{\sqrt{2}} I_a \cos\varphi = \frac{4\sqrt{3}}{\pi\sqrt{2}}\, V_d\, I_a \cos(\alpha_5)\, \cos\varphi \tag{22}$$

where $V_{ab1(1)}$ is the fundamental component of V_{ab1} and I_a is the rms value of phase a current. The active power of HB_{11} is

$$P_{\mathrm{HB11}} = \frac{V_{11(1)}}{\sqrt{2}} I_a \cos\left(\varphi + \frac{\pi}{6}\right) = \frac{4\,V_d}{3\sqrt{2}\pi}\left[\cos\left(n\alpha_2\right) + \cos\left(n\alpha_8\right) - 2\cos\left(n\alpha_5\right)\right] I_a \cos\left(\varphi + \frac{\pi}{6}\right) \quad (23)$$

where $V_{11(1)}$ is the fundamental component of V_{11}. The active power of HB_{12} is

$$P_{\mathrm{HB12}} = \frac{V_{12(1)}}{\sqrt{2}} I_a \cos\left(\varphi + \frac{\pi}{6}\right) = \frac{4\,V_d}{9\sqrt{2}\pi}\,\lambda\, I_a \cos\left(\varphi + \frac{\pi}{6}\right) \quad (24)$$

where $V_{12(1)}$ is the fundamental component of V_{12}. Then, the per-unit active power of the TTI is

$$P_{\mathrm{TTI(p.u.)}} = \frac{P_{\mathrm{TTI}}}{P_n} = \frac{\frac{4\sqrt{3}}{\pi\sqrt{2}}\,V_d\,I_a\,\cos\left(\alpha_5\right)\cos\varphi}{\sqrt{3}\,\frac{V_d}{\sqrt{2}} I_\varphi\,\cos\varphi} = \frac{4}{\pi} m \cos\left(\alpha_5\right). \quad (25)$$

The per-unit active power of HB_{11} is

$$P_{\mathrm{HB11(p.u.)}} = \frac{P_{\mathrm{HB11}}}{P_n} = \frac{\frac{4V_d}{3\sqrt{2}\pi}\left[\cos\left(n\alpha_2\right) + \cos\left(n\alpha_8\right) - 2\cos\left(n\alpha_5\right)\right] I_a \cos\left(\varphi + \frac{\pi}{6}\right)}{\sqrt{3}\frac{V_d}{\sqrt{2}} I_\varphi \cos\varphi}$$

$$= \frac{4}{3\sqrt{3}\pi}\, m\, \left[\cos\left(n\alpha_2\right) + \cos\left(n\alpha_8\right) - 2\cos\left(n\alpha_5\right)\right] \times \frac{\cos\left(\varphi + \frac{\pi}{6}\right)}{\cos\varphi}. \quad (26)$$

The per-unit active power of HB_{12} is

$$P_{\mathrm{HB12(p.u.)}} = \frac{P_{\mathrm{HB12}}}{P_n} = \frac{\frac{4\,V_d}{9\sqrt{2}\pi}\,\lambda\, I_a \cos\left(\varphi + \frac{\pi}{6}\right)}{\sqrt{3}\,\frac{V_d}{\sqrt{2}} I_{an}\,\cos\varphi} = \frac{4}{9\sqrt{3}\pi}\frac{I_a}{I_{an}}\,\lambda\,\frac{\cos\left(\varphi + \frac{\pi}{6}\right)}{\cos\varphi} = \frac{4}{9\sqrt{3}\pi} m\,\lambda\,\frac{\cos\left(\varphi + \frac{\pi}{6}\right)}{\cos\varphi}. \quad (27)$$

Replacing the values of α angles according to (15) in (16)–(27) yields the output voltages and powers of the modules in terms of m values. Similarly, the per-unit powers of HB_{21} and HB_{22} can be determined.

According to (26) and (27), the CHBs and the transformers powers are dependent on the load power factor. These equations show that $P_{\mathrm{HB11(p.u.)}}$ and $P_{\mathrm{HB12(p.u.)}}$ are functions of m and φ. The maximum value of $\cos(\varphi + \pi/6)/\cos(\varphi)$ in the $[0, \pi/3]$ interval of φ corresponds to $\varphi = 0$ in these equations. Then, the maximum values of $P_{\mathrm{HB11(p.u.)}}$ and $P_{\mathrm{HB12(p.u.)}}$ for each value of m correspond to $\varphi = 0$. Fig. 5 shows the power distribution among the modules in terms of m values according to (25), (26), and (27) for $\varphi = 0$. The output powers of the H-bridge modules are negative in some intervals. Negative power value denotes power regeneration in H-bridge. The maximum power that flows through HB_{11} and HB_{21} is 0.1 p.u. and also the maximum power that flows through HB_{12} and HB_{22} is only 0.04 p.u. Then, the total power of the transformers is 28% of the inverter rated power. The H-bridge modules and the transformers in this topology are low-rating and small size H-bridge modules and transformers, and the TTI supplies a major part of output power.

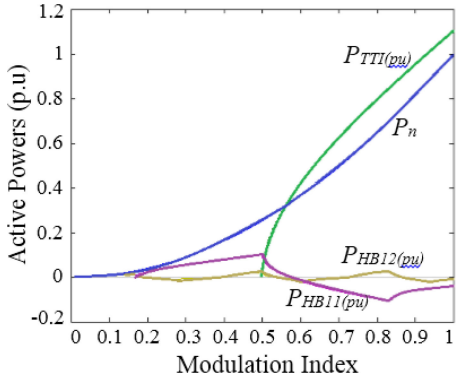

Fig. 5. Power distribution among the modules in terms of the modulation index in the proposed hybrid MLI.

D. Design Considerations of the Transformers

The transformers work with square-wave voltages and they need proportionate design considerations in some aspects. Similar to an ordinary transformer, the rated power of the transformers is a main parameter in core volume and winding calculations and design considerations. According to the power analysis, the power ratings of T_{11} and T_{21} are about 10% and the power ratings T_{12} and T_{22} are about 4% of the inverter rated power. The most important parameter is the input voltages of the transformers that have direct influence on saturation and losses. The magnetic fluxes of the transformers are the integrals of their input voltages as follows:

$$\phi(t) = \frac{1}{N_w}\int V_{in} dt \quad (28)$$

where N_w is the winding turns and V_{in} is the input voltage of each of the transformers. The cross-sectional areas of the transformers cores can be determined as follows:

$$A_c = \frac{\phi_m}{B_m} \quad (29)$$

where ϕ_m is the maximum value of the flux and B_m is the maximum flux density. According to (15), (20), (21), and (28), the fluxes of the transformers have the maximum values at $m = 0.83$. The permissible maximum flux density depends on the cores materials. The cores are ordinary steel cores and the permissible value of B_m for these cores is 1.2 wb/m^2.

The input voltages of the transformers have different harmonics components that cause eddy-current losses. The eddy-current loss density of a transformer for sinusoidal varying magnetic flux density B with frequency f is

$$P_e = K_e B^2 f^2 \quad (30)$$

TABLE III
CHARACTERISTICS OF THE SIMULATED AND IMPLEMENTED PROTOTYPE

Item	*Value*
Rated output voltage	380 V , 50 Hz
DC Source	540 V
R-L Load	R= 10 Ω , L= 21mH, cosφ = 0.84
Rated Power	S=13 kVA, P=10.9 kW, Q=7 kVAR
Transformers (Ratio , Power)	T_{11} and T_{21} : (3:1 , 1.3 KVA)
	T_{12} and T_{22} : (9:1 , 0.5 KVA)

where K_e is the eddy-crurrent constant. On the other hand, the relation between voltage and flux density is

$$V_m = 2\pi f B_m N_w A_c \tag{31}$$

where V_m is the peak value of the voltage. Then, the eddy-current loss density can be obtained as

$$P_e = K_e \left(\frac{V_m}{2\pi N_w A_c} \right)^2. \tag{32}$$

In order to reduce the eddy-current losses, the cores are laminated similar to ordinary cores. According to (15), (20), and (32), the eddy-current loss density of T_{11} related to fundamental harmonic of their input voltages for $m = 1$ is

$$P_{e1} = K_e \left(\frac{2V_d(\cos(9.6^\circ) + \cos(56^\circ) - 2\cos(30^\circ))}{3\pi^2 N_w A_c} \right)^2. \tag{33}$$

Similarly, sum of the eddy-current losses densities related to other harmonics components is

$$P_{eo} = K_e \left(\frac{2V_d}{3\pi^2 N_w A_c}\right)^2 \times \sum_{n=1}^{\infty} \frac{1}{n^2} \left[\cos\left((9.6n)^\circ\right) + \cos\left((56n)^\circ\right) - 2\cos\left((30n)^\circ\right)\right]^2. \tag{34}$$

Equation (34) shows that these losses have limited values, especially for high-order harmonics. Similarly, the eddy-current losses densities of other transformers also have limited values.

The other consideration is the average value of the input voltages of the transformers. In order to avoid dc current in the primary winding and then transformer saturation, the average value of the input voltage of the transformer must be zero. The NLM technique assures zero average value of the output voltages of the H-bridge modules.

III. SIMULATION AND EXPERIMENTAL RESULTS

The proposed MLI shown in Fig. 1 with the characteristics given in Table III was simulated and implemented. The simulations were performed using the PSCAD simulation tool and also the power analysis of the inverter was carried out in MATLAB environment. Fig. 6 shows a photograph of the prototype. Sizes of the transformers do not have much effect on bulk of the system. The dc source has been provided by a three-phase diode-bridge rectifier. The semiconductor switches are developed by LS LUH75G1202. The NLM technique has been implemented by ezDSPro F2812 board. The required drive board was designed using HCPL-316J which is a fast and intelligent IGBT driver.

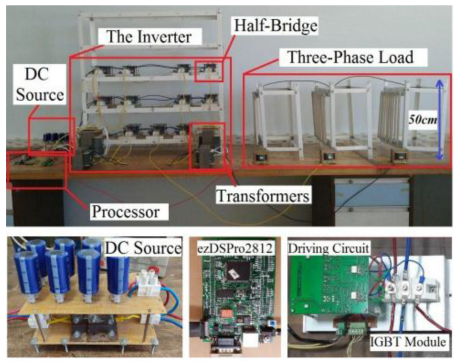

Fig. 6. Experimental setup.

The three-phase load supplied by this inverter is ohimic inductive (heating elements and inductors) with 13 kVA apparent power.

Fig. 7 shows the simulation and experimental results of the inverter. Fig. 7(a) shows the experimental line *a* to line *b* voltage (V_{ab1}) of the TTI, output voltages of HB_{11} and HB_{12} (V_{11} and V_{12}) at nominal conditions, and finally sum of these voltages that is the line *a* to line *b* voltage (V_{ab}) of the inverter. Fig. 7(b) shows the simulated output voltages of all of the modules and the output line voltages at nominal conditions in one cycle. Zero average values of V_{11}, V_{12}, V_{21}, and V_{22} are evident in Fig. 7(a) and (b). So the transformers do not have dc current saturation. The experimental three-phase output line voltages for $m = 1$ and $m = 0.8$ are shown in Fig. 7(c). Simulated phase voltages and currents of the star connected load for $m = 1$ are shown in Fig. 7(d). The total harmonic distortion (THD) values of the line voltages of the inverter in terms of the modulation index (m) are shown in Fig. 7(e). The experimental phase *a* voltage and current of the load at nominal conditions are shown in Fig. 7(f). Common-mode voltage in the proposed inverter is the voltage difference between two neutral points of the load and the dc bus of the inverter (points *o* and *n* in Fig. 1). Fig. 7(g) shows the common-mode voltage of the inverter for $m = 1$ and $m = 0.8$. The dc source of the prototype is a three-phase rectifier. The input power of the rectifier and the output power of the inverter have been measured by a three-phase power meter. The efficiency of the overall system which is the relation of the output power to the input power is 94% at nominal conditions. Fig. 8(a) shows the measured efficiency of the inverter in terms of the modulation index and the output active power. Fig. 8(b) shows the loss breakdown in different parts of the inverter at nominal conditions. The simulation and experimental results demonstrate valid performance of the proposed MLI and show that the MLI achieves balanced three-phase voltages at the *a*, *b*, and *c* terminals.

IV. FEATURES AND COMPARISONS

The sustaining voltage of the switches in the proposed MLIs is equal with the dc source voltage. The turns ratio of the transformer of the *k*th H-Bridge module is 3^k:1. So the current flowing through this module is

$$I_k = \frac{I_o}{3^k} \tag{35}$$

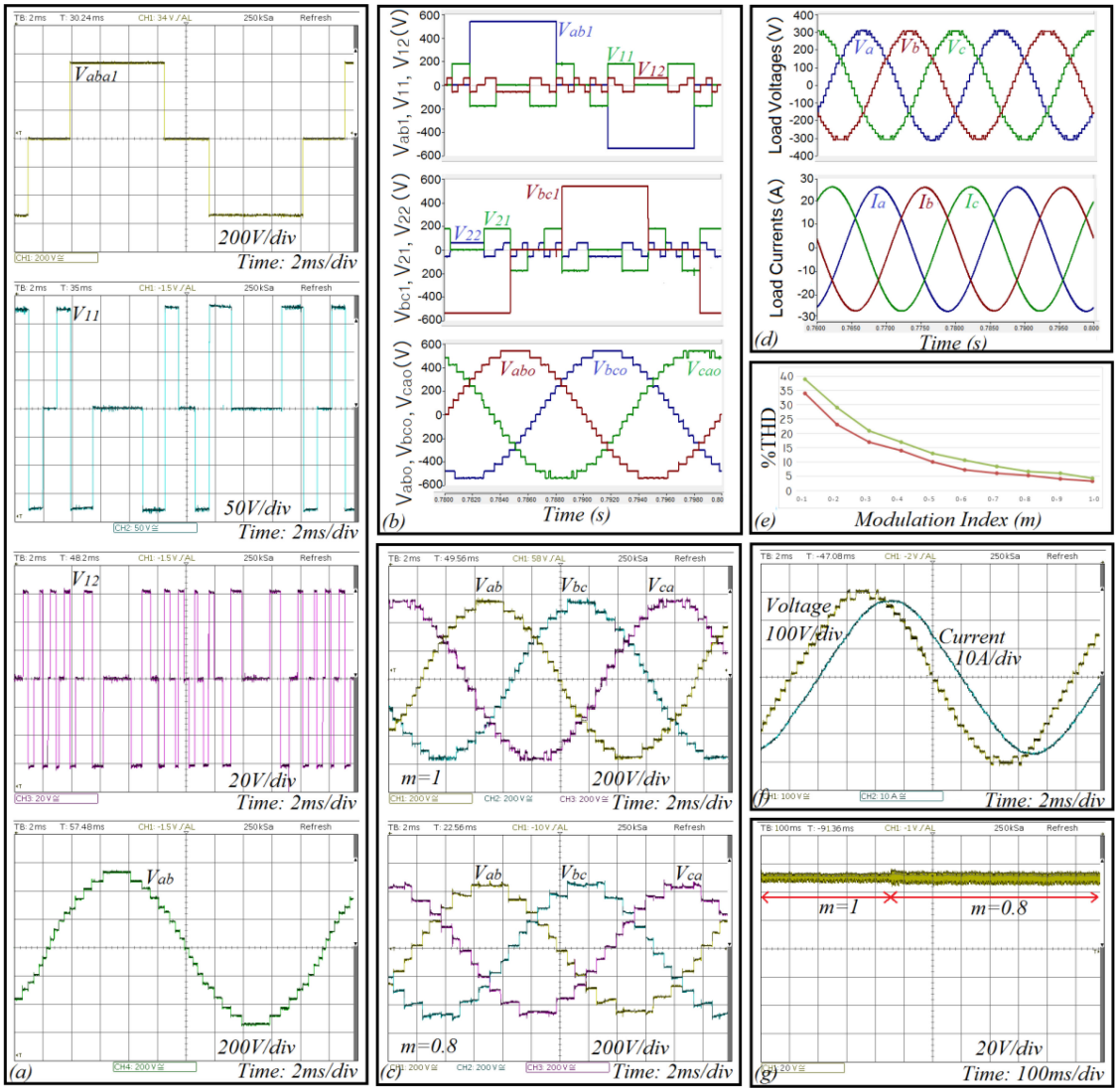

Fig. 7. Simulation and experimental results. (a) Experimental synthesize of *ab* line voltage. (b) Simulated synthesize of the output voltages. (c) Experimental line voltages for $m = 1$ and $m = 0.8$. (d) Simulated phase voltages and currents of the star-connected load for $m = 1$. (e) THD values of the line voltages in terms of m. (f) Experimental phase a voltage and current of the load at nominal conditions. (g) Common-mode voltage for $m = 1$ and $m = 0.8$.

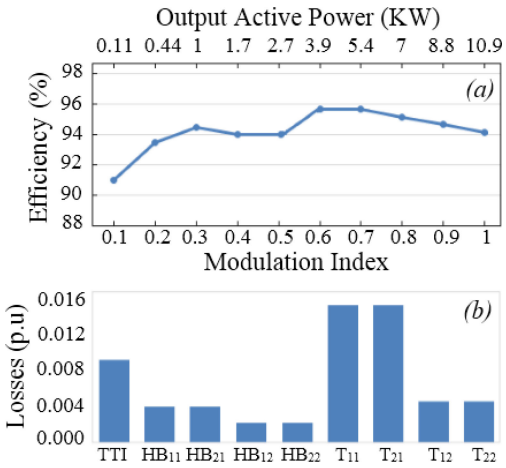

Fig. 8. (a) Measured efficiency of the inverter in terms of the modulation index and the output active power. (b) Loss breakdown in different parts of the inverter at nominal conditions.

where I_o is the output current of the inverter. As the number of the cascaded H-Bridges increases, their current ratings will be reduced in trinary manner. In the topology shown in Fig. 1, the current flowing from HB_{11} and HB_{21} modules is I_o /3 and the current flowing from HB_{12} and HB_{22} modules is I_o /9. On the other hand, the TTI module, which supplies a major part of the output power, operates at fundamental frequency and the CHBIs also have not very high switching frequencies. Therefore, the switching losses of the modules are very low and then the proposed MLI is a high efficiency converter.

Table IV gives a comparison of the proposed MLI with recently proposed advanced three-phase MLI topologies. The proposed inverter has the following advantages and disadvantages.

1) Except the topology proposed in [31], the proposed inverter has the lowest ratio of number of active switches to number of output voltage levels (R) between the compared MLIs. Notice that the inverter proposed in [31] utilizes seven dc sources. The

TABLE IV
COMPARISON AMONG THE PROPOSED HYBRID MLI AND OTHER ADVANCED THREE-PHASE MLI TOPOLOGIES

Topology proposed in	N_{VL}	N_{AS}	N_{DC}	R	N_C	$\%P_{TR}$
This paper	19	22	1	1.16	0	28%
[3]	9	18	2	2	3	-
[4]	5	16	2	3.2	0	-
[5]	5	15	1	3	3	-
[6]	25	36	4	1.44	6	-
[7]	5	18	1	3.6	4	-
[8]	19	42	3	2.21	3	-
[9]	7	24	1	3.42	5	-
[10]	5	12	1	2.4	2	100%
[11]	27	40	1	1.48	0	-
[14]	27	36	1	1.33	0	100%
[15]	19	36	1	1.89	0	100%
[16]	11	36	1	3.27	0	100%
[17]	13	48	1	3.69	0	100%
[18]	21	48	1	2.28	0	100%
[19]	9	36	1	4	0	100%
[20]	9	30	1	3.33	0	100%
[21]	9	24	3	2.66	0	100%
[27]	5	18	3	3.6	0	-
[28]	13	42	10	3.23	0	-
[29]	29	60	1	2.06	7	-
[30]	4	18	7	4.5	0	-
[31]	23	24	7	1.04	0	-

N_{VL}: number of output voltage levels; N_{AS}: number of active switches; N_{dc} : number of dc sources; N_C: number of capacitors; R: ratio of number of switches to number of output voltage levels; P_{TR}: total power of transformers (if exist).

number of driving circuitry, cost, volume, and complexity of an inverter reduce when the number of its switches and sources are reduced. This ratio shows that this inverter is an optimized inverter.

2) Similar to the proposed topology, the cascaded topology of TTI with H-bridge or half-bridge modules is proposed in [27]–[31]. In these topologies, the H-bridge or half-bridge modules are cascaded with TTI in all three phases. In the proposed topology, the H-bridges are cascaded with the TTI in two of the phases. This causes reduction in the number of the components. Moreover, the proposed topology has the advantage of utilizing only one dc source. It is an improved topology from cost and complexity aspects utilizing the lowest number of switches and sources.

3) The total power ratings of the CHBI modules in the proposed inverter are $2/\sqrt{3}$ (1.15) of total output power of CHBI modules in case of using CHBI in all three phases. Utilizing CHBI modules series connected with TTI module in all three phases causes a normal and balanced power distribution between the phases. With trinary asymmetry, the rated power of the TTI and CHMI modules is 0.69 and 0.3 of the rated power of the inverter, respectively, in this case. Then, the rated power of the CHMI is almost 0.1 of the rated power of the inverter in each phase. In the proposed topology, the power distribution is not balanced between the phases. The rated power of the TTI and CHMI modules is 0.72 and 0.28 of the rated power of the inverter, respectively. Then, each phase of the TTI supplies 0.24 of the total power and the rated power of the CHMI is 0.14 of the total power in each of the two phases. Totally, phase *a*, *b*, and *c* supply 0.38, 0.24, and 0.38 of the total power, respectively. Therefore, despite an increase equal to 0.04 of the rated power of the inverter in power ratings of the CHMIs in each phase, the number of components reduces to 2/3 in the proposed topology. From cost, bulk, and complexity aspects, the proposed topology is suitable and preferred.

4) In addition to the utilizing only one dc source, providing galvanic isolation between load and source and also using a wide range of transformer ratios are the main advantages of transformer-based single-source inverters. However, these topologies utilize bulky transformers. There is a trade-off between utilizing only one dc and utilizing bulky transformers in the proposed topology. In the proposed MLI, the TTI supplies a major part of output power and the H-bridge modules and their transformers are low power and small size modules and transformers that have no considerable effect in size, cost, and losses of the system. The proposed inverter loses the advantages of the isolation between load and source and using a wide range of transformer ratios. Nevertheless, it utilizes only one dc source with small size transformers. Then, this inverter is suitable for applications where utilizing only one dc with reduced size and cost is important than isolation or using a wide range of transformer ratios. In applications where providing galvanic isolation or using a wide range of transformer ratios is important than size and cost, a three-phase transformer can be connected to the output terminals of the TTI. And yet, the inverter takes the advantage of low ratio of number of active switches to number of output voltage levels in this condition.

5) Generally, TTIs operate by PWM methods with high switching frequencies and utilize *LC* or *LCL* passive filters at output terminals. But the proposed topology adds H-bridge converters and transformers to TTI. Obviously, the volume, cost, and complexity of these converters and transformers are higher than passive filters. However, the high switching frequency of TTIs causes high switching losses, which limits applications of these inverters, especially in high-power applications [1]. In the proposed topology, TTI operates in square-wave mode with high efficiency and the auxiliary units increase the number of voltage levels and also contribute in supplying the output power. Therefore, the proposed inverter is a suitable topology for high-power applications, especially for grid-tied applications. Moreover, similar to other MLIs, this topology has the advantages of quasi-sinusoidal output voltage with improved harmonic spectrum and lower THD and *dv/dt* compared with TTI topology. In addition, the transformers behave as low pass filters, generating a sinusoidal line current.

6) The main limitation of the proposed DCMI is the output voltage frequency. Similar to other transformer-based single-source inverters, this inverter cannot operate at wide range of frequencies because of the transformers saturations. This is a suitable candidate for constant-frequency applications like standalone and grid-tied high power quality supply systems, renewable energy sources, dynamic voltage restorers, and uninterruptible power supplies.

V. CONCLUSION

A novel hybrid MLI topology suitable for constant frequency applications is proposed in this article. A TTI is cascaded with two single-phase CHBIs at phases *a* and *c* in the proposed MLI.

It has been shown that using only two single-phase CHBIs, the MLI achieves balanced three-phase voltages at the output terminals. Reduced number of components, single dc source, and small size transformers are the three main advantages of the proposed inverter. In accordance with structure of the proposed hybrid MLI, an individual NLM method was presented and three-phase 19-level stepped sine wave output voltage has been achieved. Power distribution between its modules was analyzed and it has been shown that the H-bridge modules and the transformers are low power and small size modules and transformers. A 13-kVA laboratory prototype is implemented. Both simulation and experimental results show the validity of the proposed system.

REFERENCES

[1] H. Abu-Rub, J. Holtz, J. Rodriguez, and G. Baoming, "Medium-voltage multilevel converters—State of the art, challenges, and requirements in industrial applications," *IEEE Trans. Ind. Electron.*, vol. 57, no. 8, pp. 2581–2596, Aug. 2010.

[2] R. Agrawal and S. Jain, "Comparison of reduced part count multilevel inverters (RPC-MLIs) for integration to the grid," *Int. J. Electr. Power Energy Syst.*, vol. 84, pp. 214–224, 2017.

[3] N. Sandeep and U. R. Yaragatti, "A switched-capacitor-based multilevel inverter topology with reduced components," *IEEE Trans. Power Electron. Lett.*, vol. 33, no. 7, pp. 5538–5542, Jul. 2018.

[4] A. Hota, S. Jain, and V. Agarwal, "An improved three phase five-level inverter topology with reduced number of switching power devices," *IEEE Trans. Ind. Electron.*, vol. 65, no. 4, pp. 3296–3305, Apr. 2018.

[5] M. Norambuena, S. Kouro, S. Dieckerhoff, and J. Rodriguez, "Reduced multilevel converter: A novel multilevel converter with reduced number of active switches," *IEEE Trans. Ind. Electron.*, vol. 65, no. 5, pp. 3636–3645, May 2018.

[6] S. K. Chattopadhyay and C. Chakraborty, "Three-phase hybrid cascaded multilevel inverter using topological modules with 1:7 ratio of asymmetry," *IEEE J Emerg. Sel. Topics Power Electron.*, vol. 6, no. 4, pp. 2302–2314, Dec. 2018.

[7] M. Ghosh Majumder, A. Kumar Yadav, K. Gopakumar, K. Raj R, U. Loganathan, and L. G. Franquelo, "A five-level inverter scheme using single DC link with reduced number of floating capacitors and switches for open-end IM drives," *IEEE Trans. Ind. Electron.*, vol. 67, no. 2, pp. 960–968, 2020.

[8] F. Bahia, C. Jacobina, N. Rocha, I. Silva, and R. Sousa, "Hybrid asymmetric cascaded multilevel inverters based on three- and nine-level h-bridges," in *Proc. IEEE Trans. Ind. Appl.*, vol. 55, no. 6, pp. 6047–6060, 2019.

[9] T. Abhilash, K. Annamalai, and S. Veeramraju Tirumala, "A seven-level VSI with a front-end cascaded three-level inverter and flying capacitor fed H-bridge," in *Proc. IEEE Trans. Ind. Appl.*, vol. 55, no. 6, pp. 6073–6088, 2019.

[10] B. Satish Naik, L. Umanand, K. Gopakumar, and S. Reddy B, "A two phase five level converter with least number of power switches requiring only a single DC source," *IEEE J Emerg. Sel. Topics Power Electron.*, vol. 6, no. 4, pp. 1942–1952, Dec. 2018.

[11] J. Pereda and J. Dixon, "High-frequency link: A solution for using only one DC source in asymmetric cascaded multilevel inverters," *IEEE Trans. Ind. Electron.*, vol. 58, no. 9, pp. 3884–3892, Sep. 2011.

[12] C. Rech and J. Pinheiro Renes, "Hybrid multilevel converters: Unified analysis and design considerations," *IEEE Trans. Ind. Electron.*, vol. 54, no. 2, pp. 1092–1104, Apr. 2007.

[13] J. Singh, R. Dahiya, and L. Saini Mohan, "Recent research on transformer based single DC source multilevel inverter: A review," *Renew. Sust. Energy Rev.*, vol. 82, no. 3, pp. 3207–3224, 2018.

[14] F. Kang, S. Park, M. Lee, and C. Kim, "An efficient multilevel-synthesis approach and its application to a 27-level inverter," *IEEE Trans. Ind. Electron.*, vol. 52, no. 6, pp. 1600–1606, Dec. 2005.

[15] F. Kang, "A modified cascade transformer-based multilevel inverter and its efficient switching function," *Electr. Power Syst. Res.*, vol. 79, pp. 1648–1654, 2009.

[16] S. Song, S. Park, Y. Joung, and F. Kang, "Multilevel inverter using cascaded 3-phase transformers with common-arm configuration," *Electr. Power Syst. Res.*, vol. 81, pp. 1672–1680, 2011.

[17] A. Panda and Y. Suresh, "Research on cascade multilevel inverter with single DC source by using three-phase transformers," *Int. J. Electr. Power Energy Syst.*, vol. 40, pp. 9–20, 2012.

[18] J. Lee, H. Sim, J. Kim, and K. Lee, "Combination analysis and switching method of a cascaded h-bridge multilevel inverter based on transformers with the different turns ratio for increasing the voltage level," *IEEE Trans. Ind. Electron.*, vol. 65, no. 6, pp. 4454–4465, Jun. 2018.

[19] Y. Suresh and A. Panda, "Investigation on stacked cascade multilevel inverter by employing single-phase transformers," *Eng. Sci. Technol. Int. J.*, vol. 19, no. 2, pp. 894–903, 2016.

[20] H. Khoun Jahan, M. Naseri, M. Haji-Esmaeili, M. Abapour, and K. Zare, "Low component merged cells cascaded transformer multilevel inverter featuring an enhanced reliability," *IET Power Electron.*, vol. 10, no. 8, pp. 855–862, 2017.

[21] S. Behara, N. Sandeep, and U. Yaragatti, "Design and implementation of transformer-based multilevel inverter topology with reduced components," *IEEE Trans. Ind. Appl.*, vol. 54, no. 5, pp. 4632–4639, Sep./Oct. 2018.

[22] T. Qanbari and B. Tousi, "Transformer-based single-source multilevel inverter with reduction in number of transformers," *IJE Trans. Appl.*, vol. 29, no. 5, pp. 621–629, 2016.

[23] J. Dixon, J. Pereda, C. Castillo, and S. Bosch, "Asymmetrical multilevel inverter for traction drives using only one DC supply," *IEEE Trans. Vehic. Tech.*, vol. 59, no. 8, pp. 3736–3743, Oct. 2010.

[24] M. Moosavi and H. A. Toliyat, "A multi-cell cascaded high frequency link inverter with soft-switching and isolation," *IEEE Trans. Ind. Electron.*, vol. 66, no. 4, pp. 2518–2528, Jun. 2018.

[25] M. D. Manjrekar, P. K. Steimer, and T. A. Lipo, "Hybrid multilevel power conversion system: A competitive solution for high-power applications," *IEEE Trans. Ind. Appl.*, vol. 36, no. 3, pp. 834–841, Jun. 2000.

[26] S. Sajedi, M. Farrell, and M. Basu, "DC side and AC side cascaded multilevel inverter topologies: A comparative study due to variation in design features," *Int. J. Electr. Power Energy Syst.*, vol. 113, pp. 56–70, 2019.

[27] S. Khomfoi and C. Aimsaard, "A 5-level cascaded hybrid multilevel inverter for interfacing with renewable energy resources," in *Proc. 6th Int. Conf. Electr. Eng./Electron., Comp., Telecom. Inf. Tech.*, 2009, pp. 1–4.

[28] S. K. Chattopadhyay and C. Chakraborty, "A new multilevel inverter topology with self-balancing level doubling network," *IEEE Trans. Ind. Electron.*, vol. 61, no. 9, pp. 4622–4631, Sep. 2014.

[29] G. P. Adam, K. H. Ahmed, S. J. Finney, K. Bell, and B. W. Williams, "New breed of network fault-tolerant voltage-source-converter HVDC transmission system," *IEEE Trans. Power Electron.*, vol. 28, no. 1, pp. 335–346, Feb. 2013.

[30] A. Luiz Batschauer, S. A. Mussa, and M. Lobo Heldwein, "Three-phase hybrid multilevel inverter based on half-bridge modules," *IEEE Trans. Ind. Electron.*, vol. 59, no. 2, pp. 668–678, Feb. 2012.

[31] S. Saeidabadi, A. Ashraf Gandomi, S. H. Hosseini, M. Sabahi, and Y. Ashraf Gandomi, "New improved three-phase hybrid multilevel inverter with reduced number of components," *IET Power Electron*, vol. 10, no. 12, pp. 1403–1412, 2017.

[32] M. Sundar Manoharan, A. Ahmed, and J. Park, "A PV power conditioning system using non regenerative single-sourced trinary asymmetric multilevel inverter with hybrid control scheme and reduced leakage current," *IEEE Trans. Power Electron.*, vol. 32, no. 10, pp. 7602–7614, Nov. 2016.

[33] T. Busarello, A. Reuter, A. Péres, and M. Simões, "Understanding the staircase modulation strategy and its application in both isolated and grid connected asymmetric cascaded H-bridge multilevel inverters," *IEEE Trans. Ind. Appl.*, vol. 55, no. 5, pp. 5371–5382, Sep./Oct. 2019.

Tohid Qanbari, photograph and biography not available at the time of publication.

Behrouz Tousi received the B.Sc. degree in electronic engineering from the University of Tabriz, Tabriz, Iran, in 1988, and the M.Sc. and Ph.D. degrees in electric power engineering from the Amirkabir University of Technology, Tehran, Iran, in 1995 and 2001, respectively.

Currently, he is an Associate Professor with the Faculty of Electrical and Computer Engineering, Urmia University, Urmia, Iran. His research interests include analysis and applications of power electronics and electric power system studies.